Int. J. Exp. Path. (1997), **78,** 343–354

Vacuolar cytoplasmic phase separation in cultured mammalian cells involves the microfilament network and reduces motional properties of intracellular water

TAMÁS HENICS* AND DENYS N. WHEATLEY†

**Department of Medical Microbiology and Immunology, University Medical School of Pécs, Pécs, Hungary and †Cell Pathology Unit, University Medical School, Aberdeen U.K.*

Received for publication 21 February 1997
Accepted for publication 1 July 1997

Summary. Hep-2, human epithelial carcinoma cells, and human foreskin fibroblasts (FF9 and FF13) were exposed to either an ultrafiltrate (< 50 kD) of human sera or the weak base, procaine hydrochloride, to induce reversible cytoplasmic vacuolization. The formation of vacuoles was shown not to be due to imbibition of medium. Ultrastructural details obtained from various stages of vacuole formation were compared. In both cases of induction vacuoles were irregular and often appeared membraneless, with little in the way of electron-dense content. They started to form in the perinuclear cytoplasm and progressed towards the periphery. Osmotic stress was not involved since mitochondria remained normal throughout a vacuolization episode.

Vacuoles were often seen in close contact with filamentous structures, and this association remained detectable at late stages of the phenomenon. Fluorescent visualization of F-actin confirmed that the vacuoles were frequently bordered by microfilaments. No major metabolic impairment was apparent in vacuolized cells as judged by protein synthesis measurements, but nuclear fluorescence (DNA content) and forward light scatter (nuclear volume) by flow cytometric analysis suggested late S phase and G2 retardation. ^{1}H-nmr relaxation measurements indicated intracellular water restricted in motional characteristics in vacuolized cells. The possibility of a restricted cytoplasmic phase separation as part of a transient adaptation response is raised, and a hypothesis to explain the findings is discussed.

Keywords: cytoplasmic vacuoles, microfilament, F-actin, proton NMR, cell water, cytoplasmic phase separation

[1] Dr Tamás Henics is an International Journal of Experimental Pathology Visiting Research Fellow.

Correspondence: Dr T. Henics, Department of Medical Microbiology and Immunology, University Medical School of Pécs, Szigeti u. 12, H–7643 Pécs, Hungary. Fax: +36 72 315799, e-mail: thenics@apacs.pote.hu

An often striking and easily recognizable response of cultured cells to environmental changes is a progressive vacuolization of the cytoplasm. The inductive stimulus ranges from treatments with various drugs (Belkin *et al.* 1962; Wibo & Poole 1974; Seglen & Reith 1976; Tiganis

et al. 1992), hyperosmotic medium (Clegg *et al.* 1986; Wheatley *et al.* 1984, 1990), polyols (Nagata *et al.* 1989; Lin *et al.* 1991), weak bases (Ohkuma & Poole 1981; Finnin *et al.* 1969; Yang *et al.* 1965), bacterial toxins (Schmitt & Haas 1994; Papini *et al.* 1993; Agata *et al.* 1994; Hughes *et al.* 1988), ultrafiltrate of human sera (Henics *et al.* 1993) or retroviral infection (Weber-Benarous *et al.* 1993). In many of these cases, vacuolization occurs in a perinuclear position, which progresses towards the periphery, with increased vacuole number and size. In most instances, the phenomenon is reversible upon removal of the inducing agent. Descriptions abound, explanations are mostly speculative, and clearly any understanding of the mechanism involved is far from being reached.

The vacuolization of cells following exposure to an ultraftilrate fraction from human serum was an unexpected finding (Henics *et al.* 1993), which nevertheless has many features common with those induced by other treatments known to induce vacuolization. A major aim of the present study was to induce cytoplasmic vacuolization in various cell types with different stimuli and compare the formation and morphology of these vacuoles. We also sought to gain more information about the relationship of the induced vacuoles to cytoarchitecture, as well as an evaluation of the effects on some basic metabolic characteristics. In addition, by using ^{1}H-nmr relaxometry, we hypothesize that the vacuolization process reflects a temporary reorganization of the water within the cytoplasm, as a transient adaptation protecting the cell from further damage. In this respect it is essential to know how far the alterations can occur before the condition becomes irreversible and the cell dies. The formation and maintenance of this condition appeared to be closely related to actin-based filamental structures of the cell.

Methods

Cell cultures

Hep-2 human epithelial tumour cells and FF9 or FF13 human foreskin fibroblasts were seeded in 12-well tissue culture plates at a density of 5×10^5 cells/ml in DMEM medium supplemented with 10% foetal calf serum (FCS). Cells reached near confluency within 36 h.

Induction of cytoplasmic vacuolization

Serum ultrafiltrate was prepared as described previously (Henics *et al.* 1993). Near confluent cultures of Hep-2 or FF9 cells were exposed to ultrafiltrate of human sera (cut off value < 50 kD) in such a way that the final concentration of ultrafiltrate protein was between 125 and 300 μg/ml in the culture medium. As previously noted, the ultrafiltrate volume did not affect the osmolality of the culture medium (Henics *et al.* 1993). Vacuolization was induced by procaine hydrochloride at 1.85, 3.7 or 7.4 mM in the medium, according to Yang *et al.* (1965). Cultures were then incubated for various periods of time, and either their spontaneous reversibility was examined, or fresh media was given and the cultures likewise followed during further incubation.

Light microscopy

Cultures were examined under an inverted light microscope using phase-contrast optics. Photographs were taken at appropriate intervals to record and evaluate the size and number of vacuoles. Trypan Blue vital staining was performed after extensive washing steps in sterile PBS using 0.1% stain in serum-free DMEM for 10 min at 37°C.

Electron microscopy

Cells were fixed *in situ* in culture wells in 2.5% glutaraldehyde in serum-free medium overnight at 4°C. Post-fixation was done in 1% (w/v) OsO_4 for 1 h at room temperature, before cells were dehydrated through a series of ethanol solutions (70, 80, 95 and dry 100% v/v) and 1,2-epoxypropane. The wells were impregnated with Araldite. For final embedding, gelatin capsules were filled with fresh Araldite and inverted on to the wells. After polymerization at 60°C for 48 h, the capsules were peeled off, leaving the cells in the Araldite block. Ultrathin sections (80–90 nm) were cut using a diamond knife on a Reichert-Jung Ultracut E ultramicrotome, stained with saturated solution of uranyl acetate in 50% (v/v) ethanol for 30 min at 37°C, followed by 5 mM lead citrate for 10 min at room temperature, and examined in a Jeol 100S transmission electron microscope at an accelerating voltage of 60 or 80 kV.

Fluorescent staining and confocal microscopy

Cells were seeded and grown on 22×22 mm glass coverslips in 6-well plates and subconfluent monolayers were exposed to 3.7 mM procaine hydrochloride for 12 h. The culture medium was diluted 1:1 with PBS without Ca^{2+} or Mg^{2+} (DPBS) and the cells were incubated at 32°C for 30 min. The incubation medium was then replaced with DPBS and the cultures incubated at room temperature for a further 30 min Cells were subsequently

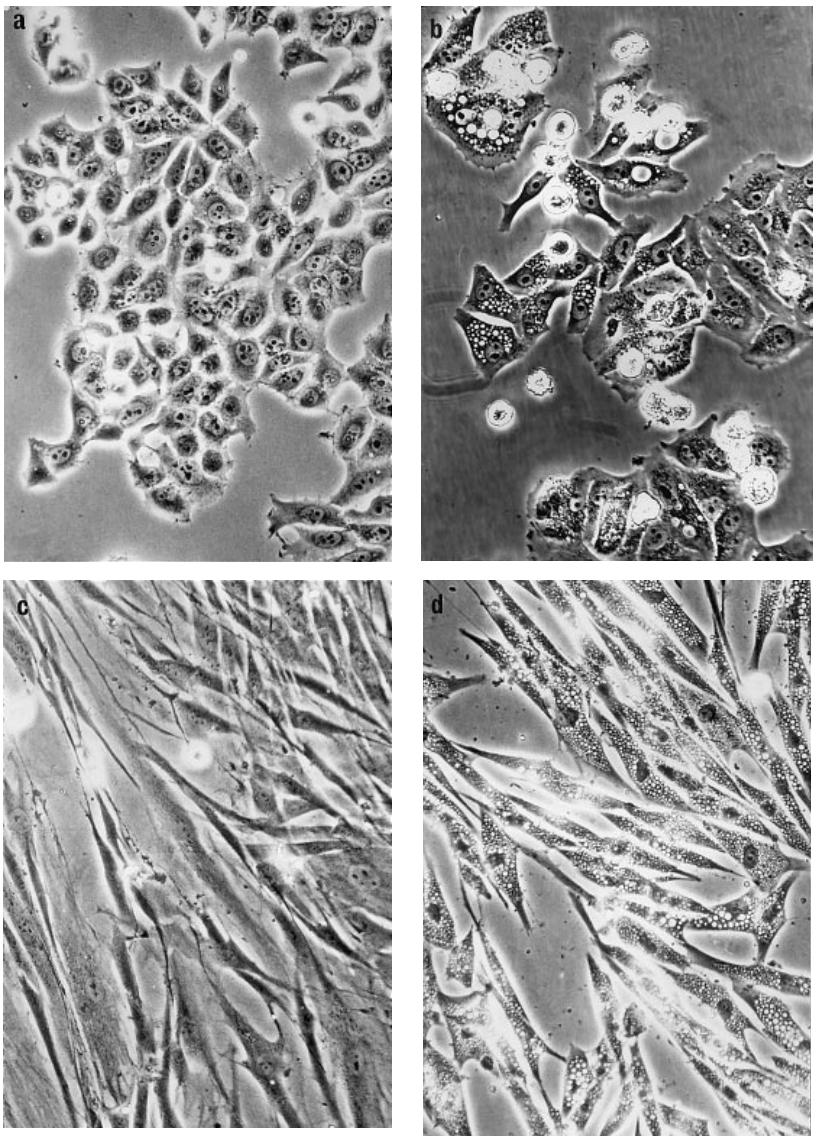

Figure 1. Light micrographs of Hep-2 (a,b) and FF-9 cells (c,d), grown in the absence (a,c) or presence (b,d) of 1.85 mM procaine-hydrochloride for 24 h. Note the presence of cytoplasmic vacuoles in procaine treated cultures. Magnification: 900x.

permeabilized with 0.5% Triton X-100 in PHEM buffer (50 mM PIPES, 25 mM HEPES, 10 mM EGTA, 10 mM $MgCl_2$) at room temperature for 2 min, washed in PHEM buffer and fixed at room temperature for 30 min in the same buffer, but containing 2% paraformaldehyde. Following incubation at 4°C overnight, cells were stained for F-actin at room temperature for 45 min with FITC-labelled phalloidin diluted 1:200 in DPBS containing 10 mg/ml BSA. After several washes in DPBS, coverslips were mounted in 2.5% DABCO reagent in 90% buffered glycerine. Slides were examined using the Olympus BH-2 fluorescence microscope with epifluorescent optics or with an MRC 600 scanning laser confocal system (Bio-Rad) fitted with a krypton/argon laser.

Cytochalasin treatment

Prior to procaine treatment, cells were exposed for 1 h to the fungal metabolite, cytochalasin D, at various concentrations to disrupt microfilaments. Cultures were then washed and treated with procaine hydrochloride, as described above, and vacuolization monitored by light microscopy.

Flow cytometric analysis

Cells were harvested by gentle trypsinization, collected by centrifugation (400 × g, 5 min) and resuspended in PBS. Nuclei were isolated and stained with propidium-iodode by the method of Vindeløv *et al.* 1983). Nuclear

fluorescence (DNA content) and forward light scatter (nuclear volume) were recorded for each population, with doublet discrimination, using an EPICS Profile-II flow cytometer (Coulter Electronics Inc., Hialeah, FL, USA). Not less than 10 000 nuclei were processed per sample. Cell cycle phase distributions were obtained by decomposition of single parameter DNA content frequency histograms using the 'Cytologic' software package peak reflection programme (Coulter Electronics Inc.).

Protein synthetic activity measurement

Cells of subconfluent monolayers were incubated in the absence or presence of procaine hydrochloride at various concentrations for 3, 6, 12 or 24 h in a 12-well plate. ^{3}H-leucine was then added to the medium at 1 μCi/ml concentration and cells were pulsed for 1 h at 37°C. Followed by washing 2x in cold PBS, cells were lysed overnight in 1N NaOH at 4°C. Incorporation was determined by normalizing measured scintillation counts for total cell protein.

^{1}H-nmr relaxometry and determination of cell water content

Measurements were done essentially as described by Wheatley *et al.* (1987). Briefly, $1–2\times10^{7}$ cells were harvested and pelleted. Pellets were centrifuged in preweighed nmr cuvettes with $3000\times$g for 2 min, the supernatant was carefully discarded, and the pellet surface was carefully wicked of any surplus fluid. Measurements were performed in a model CXP100 machine (Brueker, West Germany) at 30°C and at a frequency of 21.25 MHz. Following relaxation measurements, cuvettes were placed in an oven at 60°C for three weeks. Water contents were expressed as the percentage of wet pellet weights.

Results

Features of cytoplasmic vacuolization

When Hep-2 and FF9 or FF13 cells were exposed to medium containing either serum ultrafiltrate or the weak base, procaine hydrochloride, a dose- and time-dependent, reversible cytoplasmic vacuolization was observed

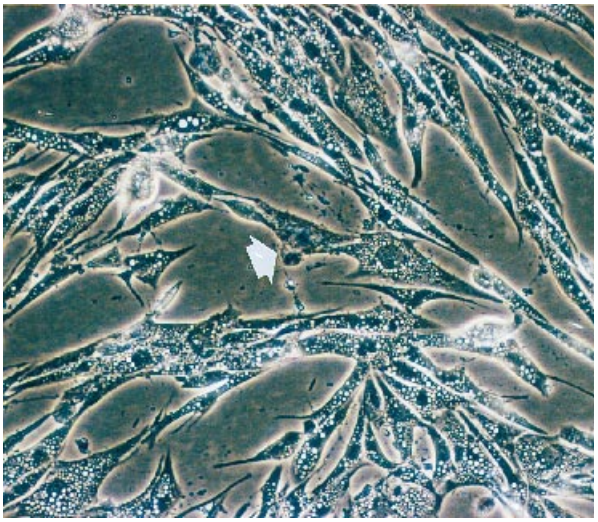

Figure 2. Trypan Blue vital staining of vacuolated FF9 fibroblast cells. Cells were exposed to 1.85 mM procaine-hydrochloride for 24 h and after wash, Trypan Blue was added to the culture in sterile PBS and cells were incubated for 10 min at 37°C. Trypan blue is excluded from the vacuolated cytoplasm. Arrow indicates a dead cell, stained blue by the vital dye. Magnification: 900x.

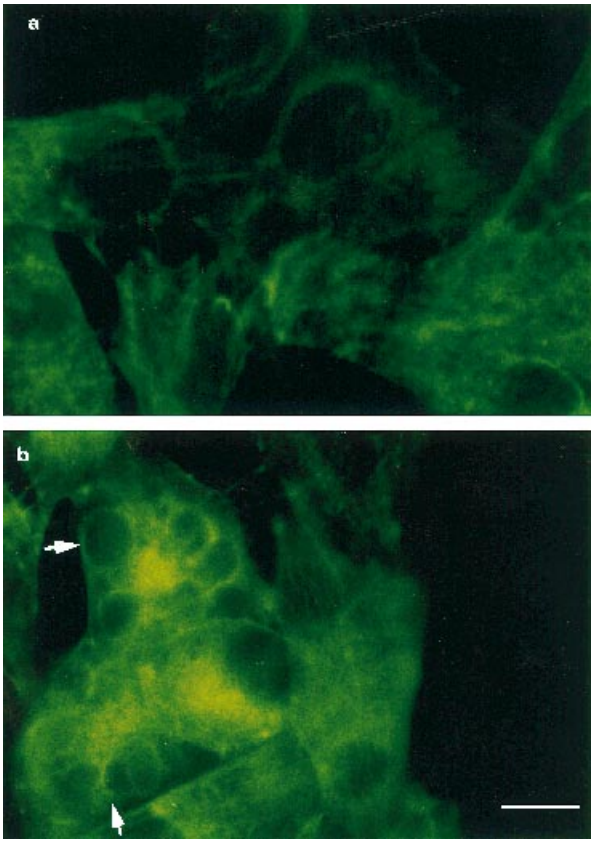

Figure 5. Fluorescent micrograph of control (a) and procaine treated (1.85 mM, 24 h, b) Hep-2 cells stained with FITC-conjugated phalloidin. Cytoplasmic vacuoles in procaine treated cells appear as actin-delineated structures (arrows). Scale bar represents 10 μm.

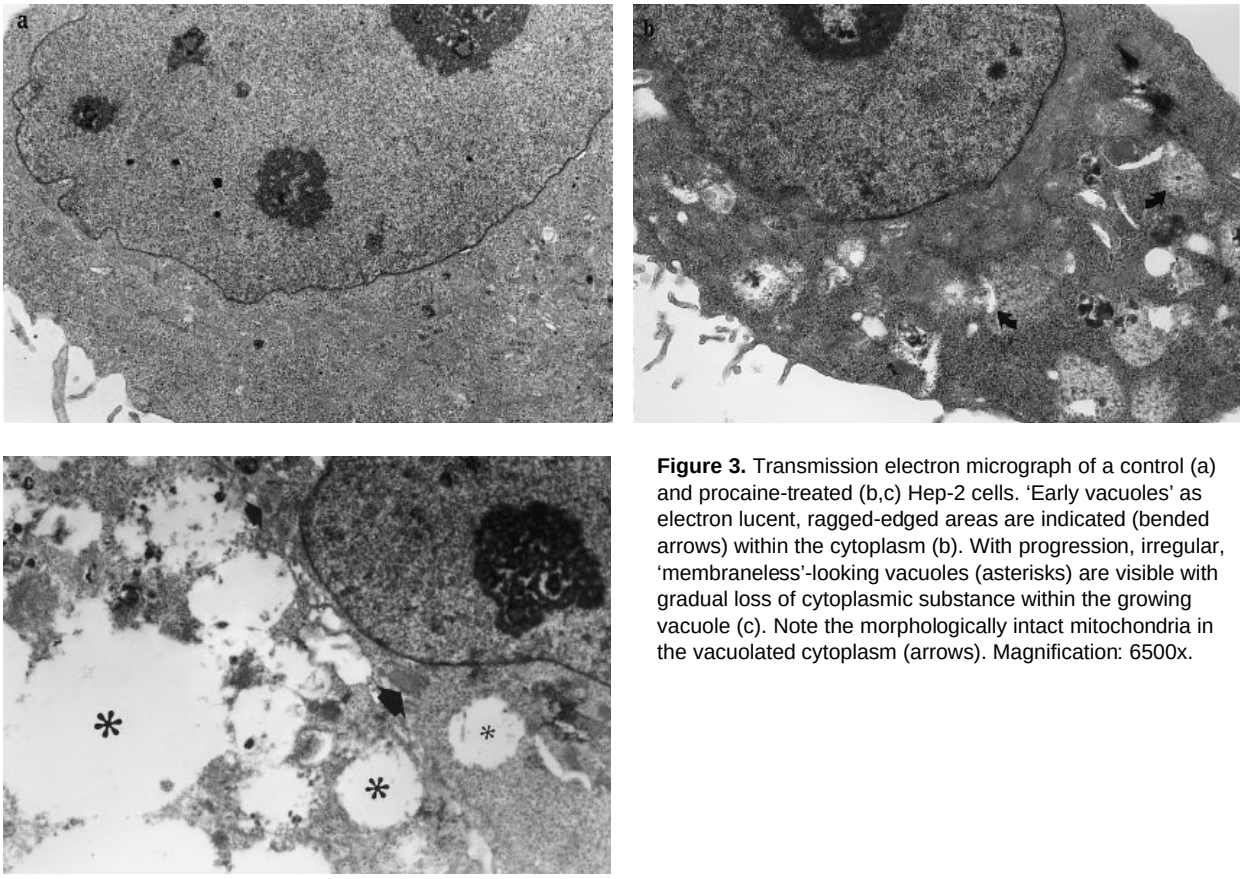

Figure 3. Transmission electron micrograph of a control (a) and procaine-treated (b,c) Hep-2 cells. 'Early vacuoles' as electron lucent, ragged-edged areas are indicated (bended arrows) within the cytoplasm (b). With progression, irregular, 'membraneless'-looking vacuoles (asterisks) are visible with gradual loss of cytoplasmic substance within the growing vacuole (c). Note the morphologically intact mitochondria in the vacuolated cytoplasm (arrows). Magnification: 6500x.

as described earlier (Yang *et al.* 1965; Henics *et al.* 1993). Figure 1 shows typical light micrographs of control and vacuolated Hep-2 (Figure 1a, b) and FF9 (Figure 1c, d) cells. Vacuoles were apparent within 1–2 h at the perinuclear region then in the more distant regions of the cytoplasm, growing in both number and size (not shown). To test if imbibition of medium was involved in the phenomenon, vacuolated cells were incubated with the vital dye, Trypan Blue. The stain was excluded from the vacuolar cytoplasm and no traces were seen in any of the vacuoles (Figure 2). Vacuolated cells showed no staining with the lipid stain Oil Red 0 (not shown).

Reversibility clearly depended upon the concentration of the drug, but in the case of ultrafiltrate of human serum, it was always a purely transient effect, as described earlier (Henics *et al.* 1993).

Ultrastructural analysis of cytoplasmic vacuoles induced by the agents

Transmission electron microscopic studies of monolayers sectioned in the plane of the coverslip revealed that the earliest alteration in certain areas of the perinuclear cytoplasmic region was disruption of the continuity of the basal cytoplasmic substance, forming an irregular electron-lucent 'space' which grew to form a vacuolar structure (Figure 3a–b). These spaces were frequently multiple, and later probably many fused together to form larger vacuoles within the cytoplasm (Figure 3b). With progression of the phenomenon, different sized vacuoles formed throughout the cytoplasm with no apparent restriction to any specific intracytoplasmic location (Figure 3c). The vacuoles contained some flocculent material in many cases, and were invariably free of lipid. They did not have the features of primary or secondary lysosomes. The inner aspect of the boundaries with the cytoplasm frequently appeared irregular, often with little obvious sign of a membrane (Figure 3c).

Parallel with these changes, one or more filament bundles were seen immediately adjacent to a forming vacuole and stayed coordinately in contact with the growing vacuoles (Figure 4a–b). As more vacuoles formed *de novo* within the cytoplasm, the filament scaffold became increasingly obvious, with additional loss of the cytoplasmic material (Figure 4c). Moreover, the only visible contact structure between two adjacent vacuoles

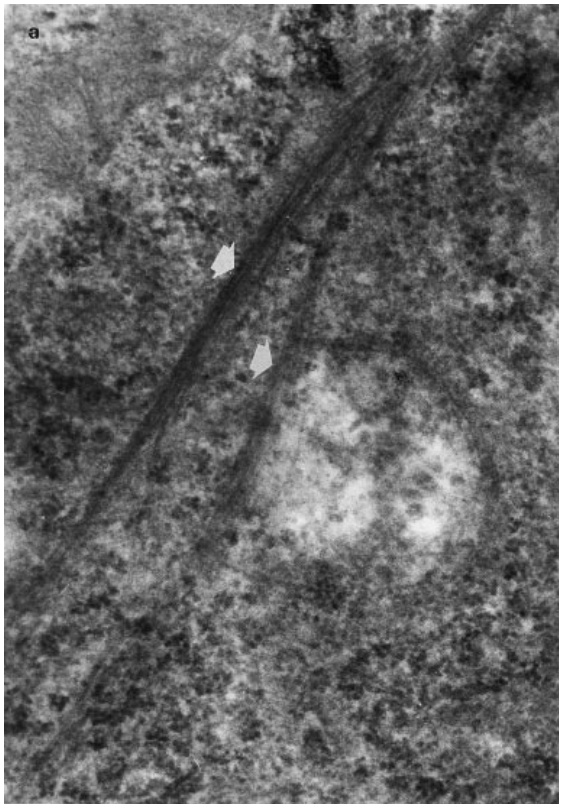
a

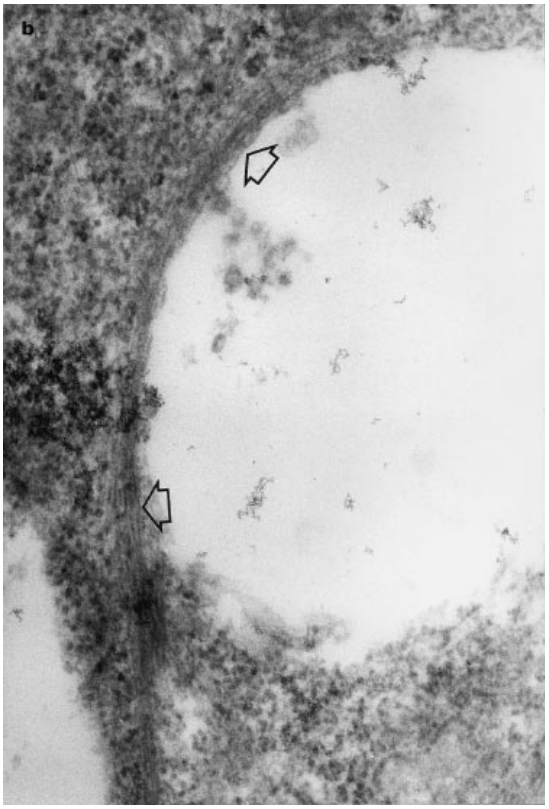
b

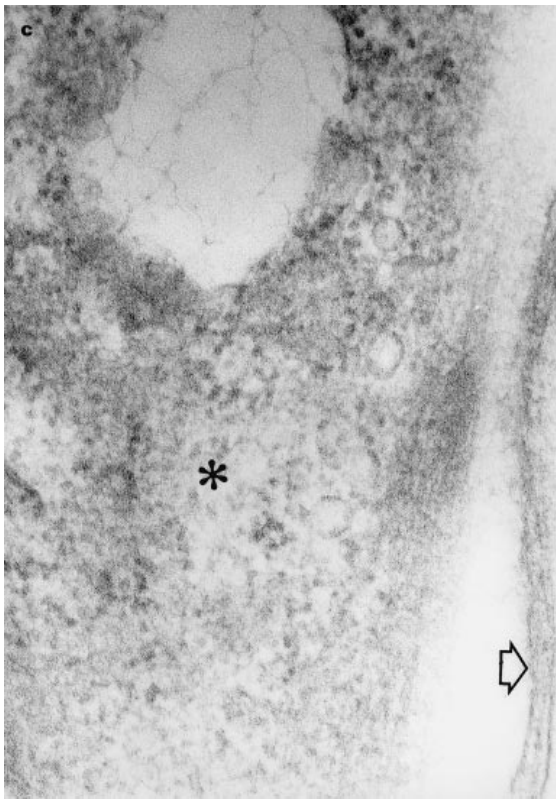
c

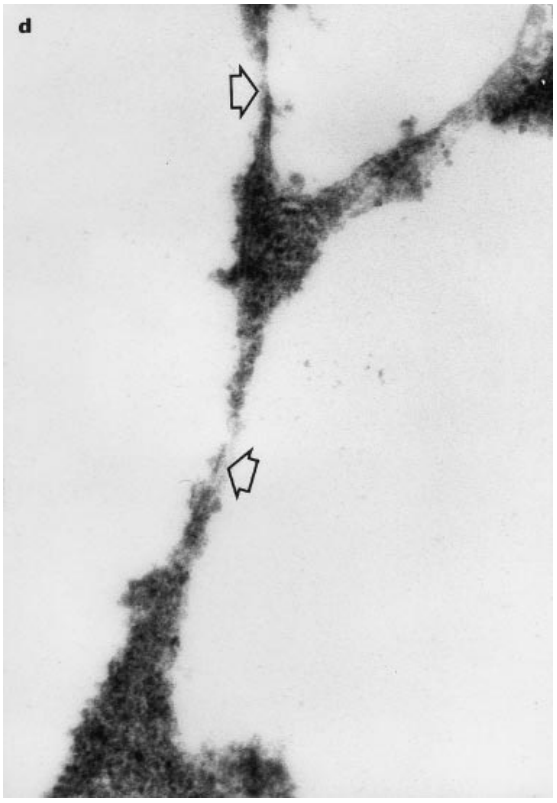
d

was a filament bundle at late stages of vacuolization, i.e. when large numbers of vacuoles occupied a substantial portion of the cytoplasm (Figure 4d).

Fluorescent visualization of microfilaments in vacuolized cells and the effect of cytochalasin D

Because vacuolated cells showed filamentous structures in close association with the cytoplasmic vacuoles, we stained cells with FITC-labelled phalloidin to visualize directly the microfilament network, often reported to be in relation with various vesicular structures (Durrbach *et al.* 1996; Murphy *et al.* 1996). Compared to control cells, where normal organization of the perinuclear and peripheral microfilaments was observed various size vacuoles were apparent with intense fluorescence in association with their surface in procaine treated cells (Figure 5). Confocal microscopic imaging also revealed that these vacuolated cells exhibited more spherical structure, judged from the fluorescent intensity in composite Z-series of 9 images. While the perinuclear actin cortex was intact, filamentous actin lined the periphery of various size vacuoles (Figure 6).

The possibility of involvement of actin filaments in the vacuolization phenomenon was supported by experiments in which the effect of cytochalasin D, a fungal microfilament disrupting metabolite, were tested on the induction process. Treatment of cells prior to the addition of procaine hydrochloride caused a dose-dependent interference with vacuole formation. Compared to control cells, cytochalasin-pretreated Hep-2 or FF13 cells had no vacuoles at higher cytochalasin doses (5–10 μM) or only a few small vacuoles at lower concentrations (0.1–1 μM; Figure 7). The retraction of cells to give the appearance seen in Figure 7c may be associated with cytoplasmic rearrangements which preclude the concomitant formation of vacuoles.

Effect of vacuolization on DNA content, cell cycle phase distribution and protein synthetic activity

In order to assess possible changes in DNA content and cell cycle distribution of vacuolated cells, we analysed intact nuclei labelled with propidium iodide as fluorochrome. Figure 8 demonstrates the result of a typical experiment where these parameters were compared in control vs. procaine-treated cells. Untreated control cells had DNA content distributions typically those of a freely cycling exponentially growing population, consistent with the recorded increase in cell number. Cells vacuolized by treatment with 1.85, 3.7 and 7.4 mM of procaine for 24 h showed altered cell cycle phase distribution. Exposure of Hep-2 cells to 1.85 mM resulted in fewer cells in S phase compared with controls, and at 3.7 mM, a definite increase in late S and G2 cells was apparent. In fibroblasts, the S phase seemed to be emptier than in controls at all dose levels, with an accumulation in late cycle stages as the concentration increased.

The often observed penetration of vacuoles into the endoplasmic reticular area suggested that protein synthetic activity of these cells might be disturbed. Figure 9 illustrates the result of a representative experiment in which cells were pulsed with ^{3}H-leucine at various times during vacuolization. These data showed no major impact of vacuole formation on overall protein synthetic activity of procaine-treated cells.

^{1}H-nmr T1 and T2 relaxation times and net water content in vacuolated cells

To determine whether the induced cytoplasmic vacuoles could originate through a mechanism that involved alterations in the physical state of intracellular water, ^{1}H-nmr T1 and T2 relaxation parameters of vacuolated cells were measured. Table 1 gives the T1 and T2 relaxation times of control and procaine-treated cells. Both relaxation parameters were significantly decreased in vacuolated cells, suggesting that the motional freedom of intracellular water is more restricted in the vacuolated state. Transmission electron microscopic examination of the same pellets revealed intact vacuoles in cells that had been prepared for the nmr measurement (not shown). Importantly, water content of vacuolated cells proved to be virtually identical to those of control cells, indicating no net loose or gain of water during vacuolization (Table 1).

Figure 4. Transmission electron micrograph of procaine-treated Hep-2 (a, b and d) and 'spontaneously' vacuolated FF9 cells (c) taken at various stages of vacuolization. Vacuoles are often in close contact with filament bundles (arrows) and these structures stay together at late phases of the phenomenon (a,b). Asterisk indicates substance-poor cytoplasm near the vacuoles (c). At late stages of the phenomenon, adjacent vacuoles often demarcated only by a filamentous structure (d, arrows). Magnification: 37 500 × (a and b), 62 500 × (c and d).

Discussion

Despite the relatively large number of reports in which extensive cytoplasmic vacuolization has been observed in response to various stimuli, little attempt has been made to monitor ultrastructural and metabolic changes in vacuolated cells. Different stimuli can lead to strikingly similar morphological responses in various cell types,

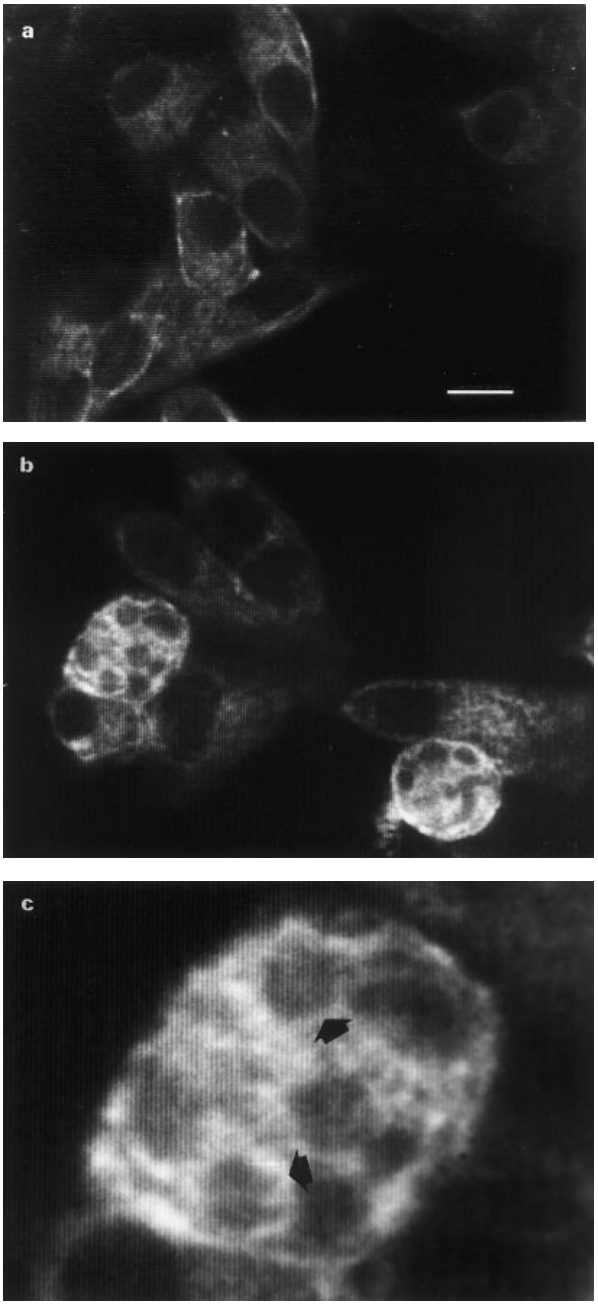

Figure 6. Confocal fluorescent micrograph of control (a) and procaine-treated (b,c) Hep-2 cells stained with FITC-phalloidin. Fluorescence was detected with a Bio-Rad MRC 600 confocal system, using 488 nm excitation wavelength and 522–558 nm emission filters. Specimens were optically sectioned by the Z series command to demonstrate intracellular structures and 9 images projected as a composite image using the COMOS software package. Vacuoles are lined around with F-actin containing structures in vacuolated cells (c, arrows). Vacuolated cells exhibit more rounded morphology. A vacuolated cell shown on the left side of panel (b) is enlarged on panel (c). Scale bar represents 10 μm.

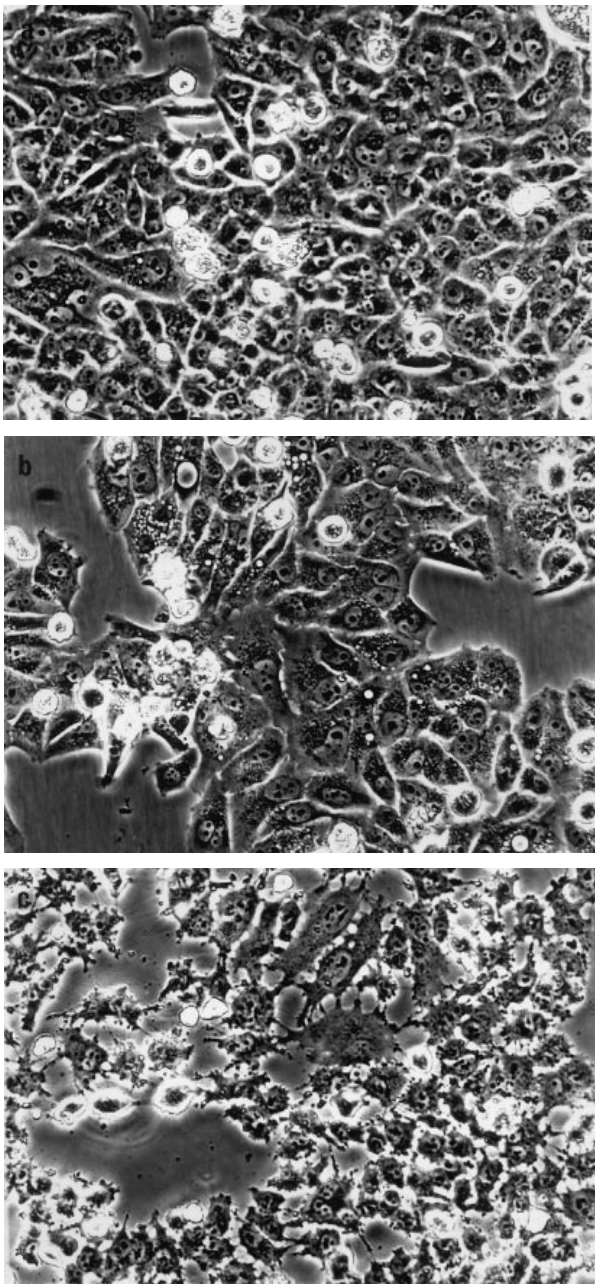

Figure 7. Light micrographs of Hep-2 cells, exposed to DMSO (vehicle control, a) or 1 (b) and 10 μM (c) cytochalasin D for 1 h prior to procaine treatment for 24 h. No differences were observed between untreated and DMSO treated cells. Note the granulation of cytoplasm at both concentrations and the ragged morphology at higher cytochalasin concentration. Few cytoplasmic vacuoles are formed at low cytochalasin doses (b) but vacuole fromation is prevented at higher concentrations (c). Magnification: 900 x.

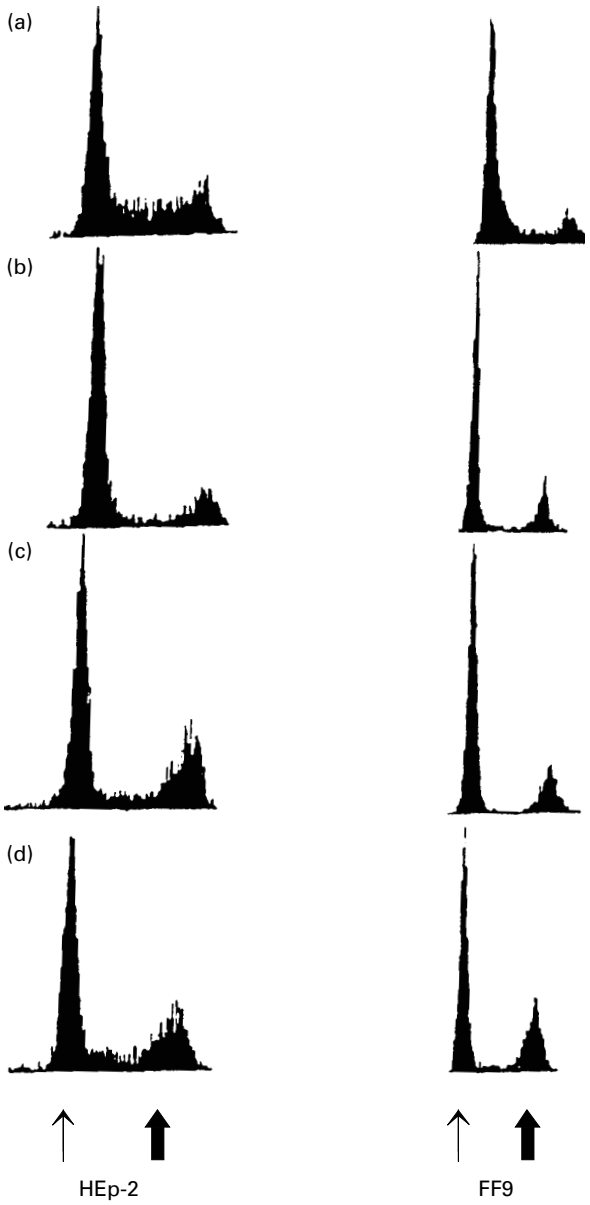

Figure 8. Histograms representing the distribution of Hep-2 and FF-9 cells through the cell cycle following treatment with procaine-hydrochloride for 24 h at various concentrations. (a) untreated control, (b) 1.85 mM, (c) 3.7 mM and (d) 7.4 mM procaine-hydrochloride treated cells. Each histogram is a plot of nuclear DNA content against frequency. ↑ represents 2n DNA content; ↑ represents 4n DNA content. These data were obtained from a single experiment but are representative of a number of independent experiments.

and therefore some form of general mechanism is mounted to such insults. The comparative work here using two distinct, but previously reported treatments, ultrafiltrate serum fractions and procaine hydrochloride, showed that the ultrastructural features of vacuoles in the two cell types were very similar. The most striking feature of these structures are their ragged-edged, *apparently* membraneless circumference and the lack of any obvious internal organization, other than some flocculent material. Further analysis indicated that the vacuoles were probably bound by a unit membrane, except this was not always visible because of the plane of the ultrathin section. Ultrastructure interpretation has been criticised and purportedly believed to be inaccurate, indeed often geometrically impossible, by Hillman & Sartory (1980); but the vacuole membrane problem has shown up the true state of affairs, since only at or near the equatorial plane of section will a membrane look like the familiar 120 Å bilipid unit. Sections cut towards the 'poles' intersect the membrane more and more tangentially, and become a foggy grayness.

The data obtained from the fluorescent and cytochalasin experiments indicate that vacuolization probably required intact microfilaments. The possible involvement of the prominent F-actin of the cytoskeleton in cannabinoid-induced vacuolization was demonstrated in cultured PC-12 cells by Wilson *et al.* (1996). Actin-microfilaments are also involved in the sorting and reorientation of endocytotic and lysosomal vesicles (Durrbach *et al.* 1996; Murphy *et al.* 1996). Segal *et al.* (1996) found epithelial cells infected by *Helicobacter pylori* to undergo prominent vacuolization with reorganization of cytoskeletal structures. It has also been shown that the agent responsible for this bacterium-induced vacuolization is a toxin, which induces strikingly similar vacuolization in Hep-2 cells to the process we have observed (Schmitt & Haas 1994; Segal *et al.* 1996). Papini *et al.* (1994) showed cytoplasmic vacuoles induced by this toxin arose from the late endocytotic compartment, but ultrastructural details were not given. Moreover, Murphy *et al.* (1996) recently found that a novel protein of the Rho family (a family of small GTPases with regulatory function on the actin-cytoskeleton) profoundly effects endosome dynamics through a microfilament-mediated mechanism. This effect, however, was distinct from any mechanism which would involve cytochalasin-sensitive structures of the actin scaffold. Thus, overall our ultrastructural data, along with the abovementioned results, indicate that our vacuoles originate from different compartments from those of endocytotic or lysosomal vesicles.

Since the vital stain, Trypan Blue, was excluded from the vacuolated cytoplasm, cells must maintain their normal permeability characteristics during vacuolization. There was no evidence of general cell swelling, as attested by the data in Table 1 on net water content, which implies no osmolar disturbance, at least at the

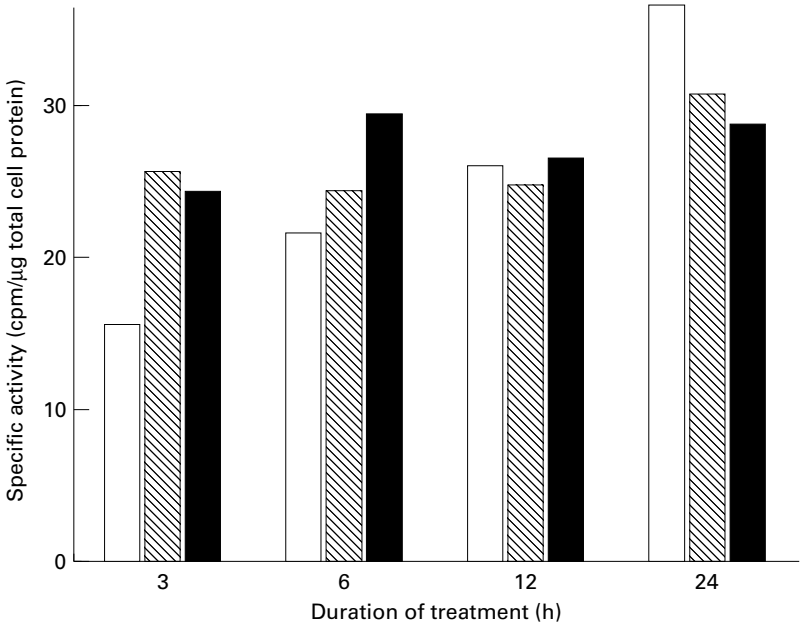

Figure 9. Tritiated leucine incorporation of Hep-2 cells exposed to two concentrations of procaine for 3, 6, 12 and 24 h. □ control, ▨ 1.85 mM procaine hydrochloride, ■ 7.4 mM procaine hydrochloride. At the end of the incubation period, cells were pulsed with 1 μCi/ml of ^{3}H-leucine for 1 h. Followed by lysis in 1N NaOH, equal aliquots of lysates were measured in a scintillation counter and assayed for protein content. Incorporation values (specific activity) are expressed as cpm per microgram of total cell protein.

whole cell level. Mitochondrial volume, cell size and internal architecture in the cytoplasm of vacuolated cells (at least prior to obvious cell demise/death) remains normal, clearly seen when such structures are juxtaposed (see Figure 3C). The flow cytometric data suggests that vacuolated cells are disturbed in their cycle progression. However, tritiated leucine pulses over a 24-h period of exposure, suggest no major changes in rate of net protein synthesis.

We observed significantly reduced ^{1}H-nmr relaxation times with no major change in net water content in vacuolated cells. The data indicate that the formation of cytoplasmic vacuoles is accompanied by a changed physical state in which the motional freedom of at least some of the cellular water is significantly reduced, but the compartment of cellular water responsible for the observed restricted motional characteristics has not been identified. At least 15% of the cell water is polarized and structured, perhaps much more, a characteristics which clearly distinguishes cell water from bulk water (Clegg 1984; Ling 1992). The idea of a microtrabecular lattice has long been proposed, which penetrates throughout the cytoplasm and serves as the framework on which glycolytic and other metabolic machinery is located (Wolosewick & Porter 1979). It has also been proposed that major basic elements of this system may provide the backbone on which a portion of cell water is structured dynamically (Clegg 1984).

In our experiments, transmission electron microscopic examination of cell pellets prepared for nmr relaxation measurements clearly verified the presence of intact vacuoles in cells with reduced proton relaxation times.

Table 1. Proton-nmr T_1 and T_2 relaxation times and net water contents of control and vacuolated Hep-2 and FF-13 fibroblast cells. Subconfluent monolayer cultures were exposed to 3.7 mM of procaine-hydrochloride for 20 or 25 h as indicated. T_1 and T_2 values were obtained using a two-parameter fitting analysis. S.D. are of four average readings. Water contents are given as a percentage of net cell pellet weight

Sample	Treatment	T_1 (ms)	S.D.	T_2 (ms)	S.D.	Water content* (%)
Hep-2	control	650.0	2.0	188.0	3.8	84.7
Hep-2	P-HCl/20 h	580.0	3.2	154.0	6.7	84.9
Hep-2	control	620.0	2.5	149.0	1.9	84.7
Hep-2	P-HCl/25 h	484.0	2.6	137.0	3.1	85.7
FF-13	control	601.0	5.0	163.0	5.1	84.3
FF-13	P-HCl/20 h	545.0	2.7	144.0	5.4	88.8

*% of wet weight.

There is some dissimilarity between the types of vacuoles in the work with hyperosomolar induction of clear vacuoles in cells, and these need to be explored and compared in much greater detail. It is possible that proteinaceous substance around the periphery or randomly distributed throughout a vacuole (seen as a flocculent content) could structure relatively large bodies of water, as epitomized by the 'watery' vacuoles in many 'mucous' secretory cells. However, these again differ in other respects from the generally clearer vacuoles we have described.

We hypothesize that vacuolization may be cytoplasmic phase-separation phenomenon, acting as an adaptive response which may permit the cell to overcome or avoid the full and perhaps fatal consequences of the various agents. Thus, full recovery can be reached upon removal of the inducer(s) with subsequent resumption of normal physiological condition, provided the vacuolization has not gone too far. Exactly what happens when the process goes too far and results in cell death has still to be explored. It is possible that at early stages of the phenomenon, active role of the filamentous protein matrix and the associated microtrabecular lattice is required to sequester cytoplasmic water in a desirable physical state. The late, extreme phases, when the process is no longer reversible, may indicate that the capacity of the cell to 'sacrifice' further cytoplasmic substance is exhausted. Vacuoles intermittently fuse together and expansion occurs. Transition areas between filament bundles and the lattice might be the last elements surviving the disrupting forces implemented by the expanding vacuoles.

In conclusion, we emphasize the possibility that the often observed cytoplasmic vacuolization of cultured mammalian cells may be a general phenomenon which involves elements of basic cytoplasmic organization, the physiological mechanisms and consequences of which need much more detailed explanation. Further studies are being carried out to establish whether the process of cytoplasmic phase separation is occurring, as well as to improve the characterization of the role of cytomatrix elements in this process.

Acknowledgements

This work was carried out during tenure of an International Journal of Experimental Pathology Research Fellowship to TH. We are grateful to Dr Margaret Foster for providing us with the facilities for the nmr measurements. The excellent technical help of Yiannis Seimenis is appreciated. We would also wish to thank Janet Liversidge for her help in the confocal microscopic studies.

References

Agata N., Mori M., Ohta M., Suwan S., Ohtani I. & Isobe M. (1994) A novel dodecadepsipeptide, cereulide, isolated from *Bacillus cereus* causes vacuole formation in Hep-2 cells. *FEMS Microbiol. Lett.* **121,** 31–34.

Belkin M., Hardy W.G., Orr H.C. & Lachman A.B. (1962) Induction *in vitro* by autonomic drugs of cytoplasmic vacuoles in ascites tumor cells. *J. Nat. Cancer Inst.* **28,** 187–201.

Clegg J.S. (1984) Properties and metabolism of the aqueous cytoplasm and its boundaries. *Am. J. Physiol.* **246,** R133–R151.

Clegg J.S., Gallo J. & Gordon E. (1986) Some structural, biochemical and biophysical characteristics of l-929 cells growing in the presence of hyperosmotic sorbitol concentrations. *Exp. Cell Res.* **163,** 35–46.

Durrbach A., Louvard D. & Coudrier E. (1996) Actin filaments facilitate two steps of endocytosis. *J. Cell. Sci.* **109,** 457–465.

Finnin B.C., Reed B.L. & Ruffin N.E. (1969) The effects of osmotic pressure on procaine-induced vacuolation in cell culture. *J. Pharm. Pharmac.* **21,** 114–117.

Henics T., Kõszegi T., Szûcs G.Y., Kellermayer M.S.Z. & Kellermayer M. (1993) Transient cytoplasmic vacuolization in cultured normal and neoplastic cells treated with low molecular weight human serum ultrafiltrate: Is out inside? Physiol. *Chem. Phys. & Med. NMR* **25,** 227–236.

Hillman H. & Sartory P. (1980) The living cell: a re-examination of its fine structure. Chichester: Packard Publishing, Ltd., pp. 35–78.

Hughes S., Bartholomew B., Hardy J.C. & Kramer J.M. (1988) Potential application of a Hep-2 cell assay in the investigation of *Bacillus cereus* emetic-syndrome food poisoning. *FEMS Microbiol. Lett.* **52,** 7–12.

Lin L.-R., Reddy V.N., Giblin F.J., Kador P.F. & Kinoshita J.H. (1991) Polyol accumulation in cultured human lens epithelial cells. *Exp. Eye Res.* **52,** 92–100.

Ling G.N. (1992) A revolution in the physiology of the living cell. Malabar: Krieger Publishing Company. pp. 69–110.

Murphy C., Saffrich R., Grummt M., Gournier H., Rybin V., Rubino M., Auvinen P., Lutcke A., Parton R.G. & Zerial M. (1996) Endosome dynamics regulated by a Rho protein. *Nature* **384,** 427–432.

Nagata M., Hohman T.C., Nishimura C., Drea C.M., Oliver C. & Robinson W.G. (1989) Polyol and vacuole formation in cultured canine lens epithelial cells. *Exp. Eye Res.* **48,** 667–677.

Ohkuma S. & Poole B. (1981) Cytoplasmic vacuolation of mouse peritoneal macrophages and the uptake into lysosomes of weakly basic substances. *J. Cell Biol.* **90,** 656–664.

Papini E., De Bernard M., Milia E., Bugnoli M., Zerial M., Rappuoli R. & Montecucco C. (1994) Cellular vacuoles induced by *Helicobacter pylori* originate from late endosomal compartments. *Proc. Natl. Acad. Sci. USA* **91,** 9720–9724.

Papini E., Bugnoli M., De Bernard M., Figura N., Rappuoli R. & Montecucco C. (1993) Bafilomycin A1 inhibits *Helicobacter pylori*-induced vacuolization of HeLa cells. *Molec. Microbiol.* **7(2),** 323–327.

Schmitt W. & Haas R. (1994) Genetic analysis of the *Helicobacter pylori* vacuolating cytotoxin: structural similarities with the IgA protease type of exported protein. *Molec. Microbiol.* **12(2),** 307–319.

Segal E.D., Falkow S. & Tompkins L.S. (1996) *Helicobacter pylori* attachment to gastric cells induces cytoskeletal rearrangements

and tyrosine phosphorylation of host cell proteins. *Proc. Natl. Acad. Sci. USA* **93,** 1259–1264.

SEGLEN P.O. & REITH A. (1976) Ammonia inhibition of protein degradation in isolated rat hepatocytes. *Exp. Cell Res.* **100,** 276–280.

TIGANIS T., LEAVER D.D., HAM K., FRIEDHUBER A., STEWART P. & DZIADEK M. (1992) Functional and morphological Changes induced by tunicamycin in dividing and confluent endothelial cells. *Exp. Cell Res.* **198,** 191–200.

VINDELØV L.L., CHRISTENSEN I.J. & NISSEN N.I. (1983) A detergent-trypsin method for the preparation of nuclei for flow cytometric DNA analysis. *Cytometry* **3,** 323–327.

WEBER-BENAROUS A., DECAUX J.F., BENNOUN M., ALLEMAND I., BRIAND P. & KAHN A. (1993) Retroviral infection of primary hepatocytes from normal mice and mice transgenic for SV40 large T antigen. *Exp. Cell Res.* **205,** 91–100.

WHEATLEY D.N., INGLIS M.S. & CLEGG J.S. (1984) Dehydration of HeLa S-3 cells by osmosis. 1. Kinetics of cellular responses to hypertonic levels of sorbitol, amino acids and other selected agents. *Molec. Physiol.* **6,** 163–182.

WHEATLEY D.N., INGLIS M.S., FOSTER M.A. & RIMINGTON J.E. (1987) Hydration, volume changes and nuclear magnetic resonance proton relaxation times of HeLa S-3 cells in *M*-phase and the subsequent cell cycle. *J. Cell Sci.* **88,** 13–23.

WHEATLEY D.N., RIMMINGTON J.E. & FOSTER M.A. (1990) Effects of osmotic manipulation of intracellular hydration of HeLa S-3 cells on their proton NMR relaxation times. *Magn. Reson. Imaging* **8,** 285–293.

WIBO M. & POOLE B. (1974) Protein degradation in cultured cells. II. The uptake of chloroquine by rat fibroblasts and the inhibition of cellular protein degradation and cathepsin B1. *J Cell Biol.* **63,** 430–440.

WILSON R.G. JR, TAHIR S.K., MECHOULAM R., ZIMMERMAN S. & ZIMMERMAN A.M. (1996) Cannabinoid enantiomer action on the cytoarchitecture. *Cell Biol. Internatl.* **20,** 147–157.

WOLIN S.L. & KUCHERLAPATI R.S. (1979) Expression of microtubule networks in normal cells, transformed cells, and their hybrids. *J. Cell Biol.* **82,** 76–85.

WOLOSEWICK J.J. & PORTER K.R. (1979) Microtrabecular lattice of the cytoplasmic ground substance: artifact or reality? *J. Cell Biol.* **82,** 114–139.

YANG W.C.T., SRASSER F.F. & POMERAT C.M. (1965) Mechanism of drug-induced vacuolization in tissue culture. *Exp. Cell Res.* **38,** 495–506.